DOR: 20.1001.1.27170314.2021.10.1.4.3

Research Paper

# Investigation of the Effect of Different Forming Pressure Curves on Formability of AA1050 Tubes in Warm Hydroforming Process

**Seyed Jalal Hashemi**[1*]

[1]Department of Mechanical Engineering, Faculty of Enghelab-e Eslami, Tehran Branch, Technical and Vocational University (TVU), Tehran, Iran

[*]Email of Corresponding Author: j_hashemi@tvu.ac.ir

*Received: March 6, 2021; Accepted: May 27, 2021*

**Abstract**

Reduction of weight and increase of corrosion resistance are among the advantages of applications of aluminum alloys in the automotive industry. Low formability at room temperature is the major problem in the forming of these alloys. This problem is due to alloy elements that limit the number of slip planes at room temperature. Forming at a high temperature can improve the formability of metals. In this paper, the warm hydroforming of AA1050 aluminum tubes has been studied numerically. A warm tube hydroforming setup was designed and fabricated. Aluminum tubes were formed at high temperatures. Numerical simulation of process is performed using MSC. Marc commercial software and thickness distribution were studied at various temperatures. Results showed that increasing temperature leads to a much better thickness distribution. The pressure curves which were obtained using available equations for forming at room temperature have been modified to decrease thinning in the final part. Simulations were performed in two states which are called constrained bulge and free bulge. To produce a part without any wrinkling and also to obtain minimum thinning, an axial feeding curve is suggested.

**Keywords**

Warm Tube Hydroforming, Finite Eelement Method (FEM), Aluminum Alloy

## 1. Introduction

The tube hydroforming process is one of the sheet metal forming processes that are used considerably in the automobile industry. In tube hydroforming, extruded tubes or seamless tubes are formed into complicated parts. In this process, the shape of the cavity is imposed on the initial tube using internal pressure. Axial feeding is an auxiliary tool to facilitate deformation and material plastic flow. High strength aluminum and magnesium alloys, with a good strength per weight ratio, can replace steel alloy in automobile components. Low stiffness and low formability are the main problems of these alloys. Increasing process temperature can improve the formability of the metals. Warm hydroforming has many advantages such as the capability of forming complicated components, lower force and forming pressure, and smaller dies setup. Nowadays, the maximum temperature of the hydroforming process is 300 ˚C. There is no appropriate fluid for warm hydroforming which can work well up to 300 ˚C. Lee et al. [1] investigated hydro-formability of AA7075 aluminum tubes at

temperatures between room temperature to warm temperature near 300 ˚C. In their study, the die was warmed using a heating element that was located in the fluid. After reaching the temperature of the die to the desired point, the process started. Based on the results, more hydro-formability can obtain with increasing process temperature.

Yuan et al. [2] studied the effect of temperature on mechanical properties of 4A02 aluminum tubes in tube hydroforming and uniaxial tensile test. Results of both tests showed that elongation and hydro-formability of tubes increases at high temperatures and the maximum of the bulge is obtained at temperatures between 200 ˚C and 300 ˚C. Kim et al. [3] simulated a free bulge test of AA6061 tubes at high temperatures using DEFORM-2D software. Yi et al. [4] designed and fabricated a combined heating system of tube hydroforming. Using this heating system, temperature distribution on the tube is more uniform than in old systems. Hashemi et al. [5] studied the thickness distribution of hydroformed aluminum tubes AA1050 at high temperatures and found that the temperature uniforms the thickness distribution by decreasing the thinning of bend areas. Seyedkasi et al. [6] investigate the optimization of forming conditions of aluminum tubes at high temperatures. Hashemi et al. [7] used ductile fracture criteria to predict tube bursting in warm hydroforming of AA6063 tubes. Taheri Ahangar et al. [8] design a new die for decreasing the corner radius of stepped tubular parts in warm tube hydroforming. Reddy et al. [9] used different heat treatments to increase the formability tubes in free bulge hydroforming. Zhang et al. [10] use the response surface method (RSM) to optimize the loading path in the tube hydroforming process. Taheri Ahangar et al. [11] simulated the tube hydroforming process at high temperatures and studies the effect of forming parameters of wrinkling and bursting of tubes. Nasrollahzade et al. [12] investigated forming of aluminum tubes at high temperatures using got metal gas forming process.

Selecting loading curves is the most important parameter in tube hydroforming design. If an appropriate loading curve is selected, a part without wrinkling and thinning can be produced. In this paper, coupled thermomechanical simulation of the warm tube hydroforming process is performed to obtain an appropriate loading curve.

## 2. Tube properties

The chemical composition of tube material is shown in Table 1. Among all-alloy elements, Fe and Si have more effect on decreasing the formability of this alloy at room temperature. According to composition, this material is about AA1050 alloy.

A uniaxial tensile test was carried out at various temperatures between room temperature to 290 ˚C. Uniaxial tensile test samples were prepared according to the ASTM-E8M standard. As predicted for metals, increasing temperature lead to increasing yield stress. Stress-strain curves at various temperatures are shown in Figure 1.

Table 1: Chemical composition of the tube

| Al | Mg | Cu | Mn | Fe | Si | Ni | Ti |
|---|---|---|---|---|---|---|---|
| Balance | 0.08 | 0.015 | 0.01 | 0.15 | 0.14 | 0.01 | 0.02 |

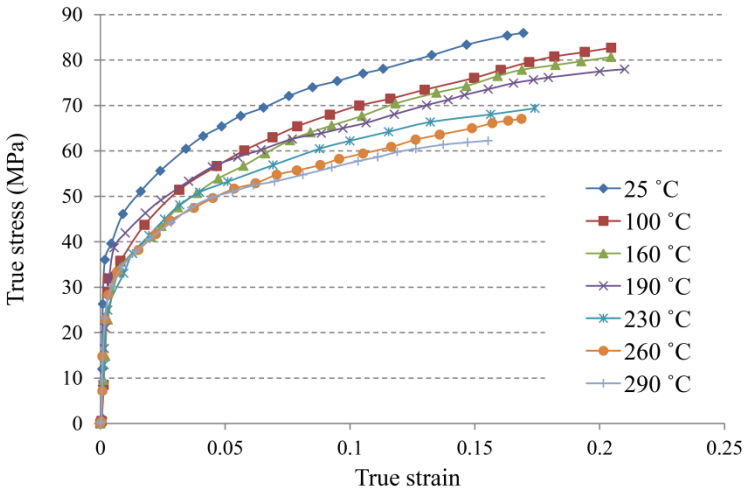


Figure 1. Stress-strain curves at various temperatures

## 3. FEM simulation

In order to identify the deformation behavior of the aluminum tubes during the warm tube hydroforming, finite element simulation of this process was carried out using MSC. Marc Mentat software. To simulate the forming pressure effect, a uniform pressure distribution was imposed on the inner surface of the tube. To decrease the simulation time cost, one-quarter of the tube and die were modeled. Tube and die models are shown in Figure 2.

Other parameters of the tube are given in Table 2. Die surfaces were considered completely rigid and the tube surface was divided into 1275 shell elements. The elements are referred to with number 139 in MSC. Marc Mentat element library is four-node thin shell elements and bilinear interpolation is used for the coordinates, displacements, and rotations. These elements can be used in curved shell analysis (MSC.Marc Mentat help) as well as tube hydroforming simulation. Because of the small tube volume, compared to that of the die, and the high heat conductivity of the tube, it is logical to consider the tube temperature constant. The friction condition between the outer surface of the tube and the inner surface of the die cavity was modeled using Coulomb's law and friction coefficient of 0.1.

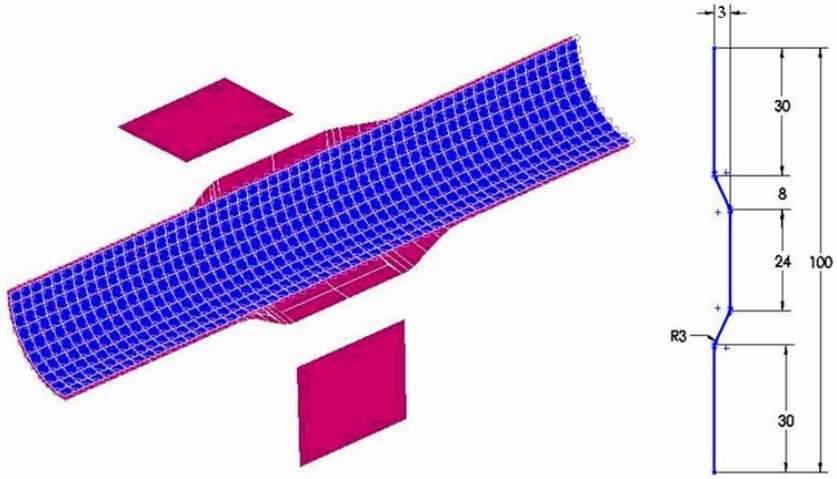


Figure 2. Simulation model

Table 2. Material and process parameters

| Parameter | Amount |
|---|---|
| Equipment | |
| Initial tube diameter (mm) | 24 |
| Initial tube thickness (mm) | 1 |
| Tube temperature (°C) | 100, 160, 230 |
| Mechanical characteristics | |
| Young modulus (GPa) | 70 |
| Poisson ratio | 0.3 |
| Thermal characteristics | |
| Heat conductivity coefficient of tube (W/m.k) | 220 (AS.M Handbook) |
| Specific heat capacity of tube (J/kg.K) | 904 (ASM Handbook) |

The primary pressure curve is obtained using equations that exist for room temperature. Yield pressure, forming pressure and calibration pressure is calculated using equation (1), (2) and (3) respectively [6]:

$$P_{iy} = \sigma_y \frac{2t_0}{D_0 - t_0} \quad (1)$$

$$P_{ib} = \sigma_{uts} \frac{2t_0}{D_0 - t_0} \quad (2)$$

$$P_{i\max} = \frac{2}{\sqrt{3}} \sigma_{uts} \left[ \ln \frac{R}{R - t_0} \right] \quad (3)$$

In these equations, $\sigma_y$ and $\sigma_{uts}$ are yeild and ultimate stress of the material. $t_0$ is the thickness of the tube before forming process. $D_0$ and $R$ are the primary diameter of the tube and corner radii of the die, respectively. Importing yield and ultimate stress at 100 ˚C, 160 ˚C, and 230 ˚C into these equations, primary pressure curves at mentioned temperatures are obtained as shown in Figure 3.

## 4. Laboratory setup

A laboratory setup was designed and fabricated to verify FEM results. This setup can control internal pressure, axial feeding, and process temperature. The setup is shown in Figure 4.

Two hydraulic pumps were used to control internal pressure and axial feeding simultaneously.

Eight cartridge heating elements were inserted into the upper and lower caps of the die. These elements were used to heat the die and tube to the desired temperature. The fluid temperature was monitored using one thermocouple type K which was installed at the tip of one of the axial feeding punches. The layout of the heating elements and thermocouple is shown in Figure 5 schematically.

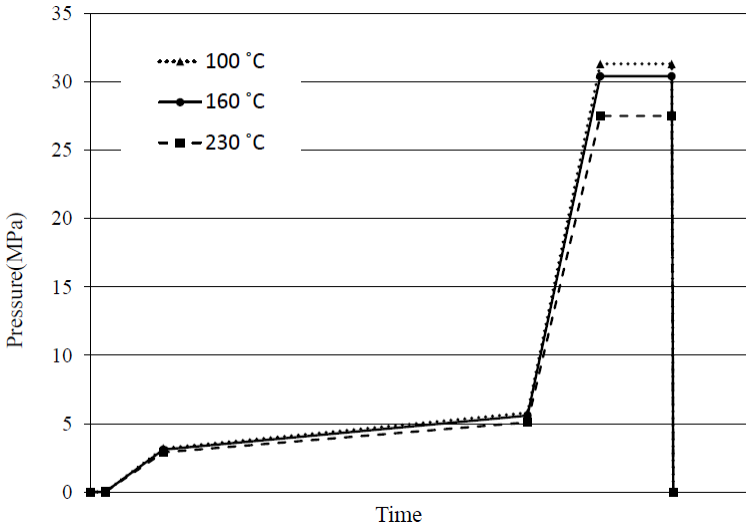


Figure 3. Primary pressure curve at 100˚C, 160 ˚C, and 230˚C

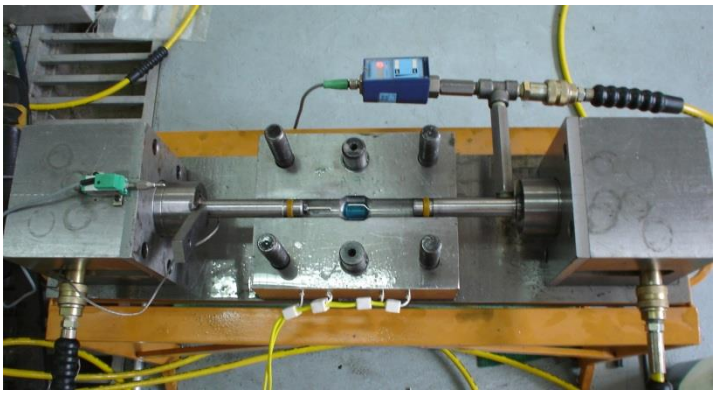

Figure 4. Laboratory setup

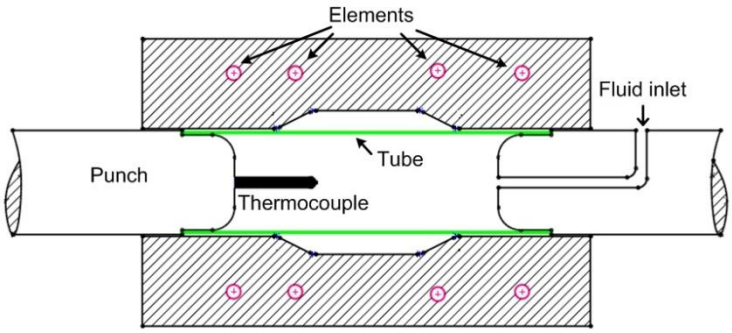


Figure 5. The layout of heating elements and thermocouples in the upper and lower caps of the die

In experiments, firstly, axial feeding punches seal tube ends. After sealing, the tube is filled with fluid at room temperature and then elements heat the die. When the temperature of fluid reaches the desired point, the pressure curve is applied to the tube using hydraulics pumps.

## 5. Results and Discussions

Primary pressure curves at each temperature are changed to obtain minimum thinning in two states of the free bulge and constrained bulge. In a free bulging case, the ends of the tube can move freely.

The only parameter which limits the tube deformation is the friction of die and tube surfaces. In constrained bulge cases, both ends of the tube are fixed and axial feeding is disregarded. In this case, the flow of the material is concentrated in deformation zones near the corners. Since increasing the process temperature leads to material softening, necking, and thinning happen sooner than lower temperatures in the corners.

Figure 6 (a) is shown a set of pressure curves which are obtained by changing the primary pressure curve at 100 ˚C slightly. Thinning is obtained by equation (4):

$$thinning\ (\%) = \frac{t - t_0}{t_0} \times 100 \qquad (4)$$

$t$ is the minimum thickness of the formed tube. Pressure curves which are shown in Figure 6 (a) applied on the internal tube surface in simulation. Maximum thinning of formed part subjected to all pressure curves, in two states of the constrained and free bulge, is shown in Fig. 6 (b). Among these pressure curves which are used at 100 ˚C, C15-100 has minimum thinning but the calibration pressure of this curve is not enough to form part in die corner.

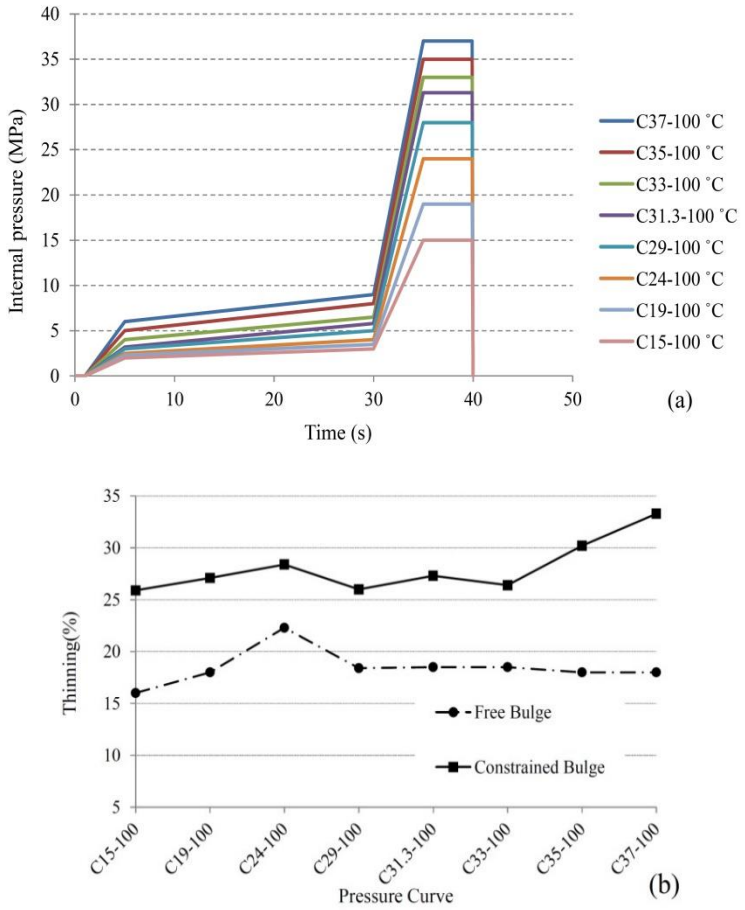


Figure 6. (a) Pressure curve using at 100 ˚C (b) maximum thinning using new pressure curves

For C35-100 and C37-100 pressure curves, equivalent stress exceeds the ultimate stress of material at 100 ˚C; therefore, the probability of bursting is very high. Considering the minimum thinning for the final part, the C29-100 pressure curve was selected at this temperature.

New pressure curves at 160 ˚C were obtained with changing primary pressure curves at this temperature like 100 ˚C. These pressure carves are shown in Figure 7 (a).
Considering simulation results which are shown in Figure 7 (b), C28-160 was selected. Using this pressure curve, minimum thinning was obtained at 160 ˚C.
Like 100 ˚C and 160 ˚C, the primary pressure curve was changed at 230 ˚C. New pressure curves are shown in Figure 8 (a). To minimize the thinning, C20-230 was selected between these pressure curves at 230 ˚C.

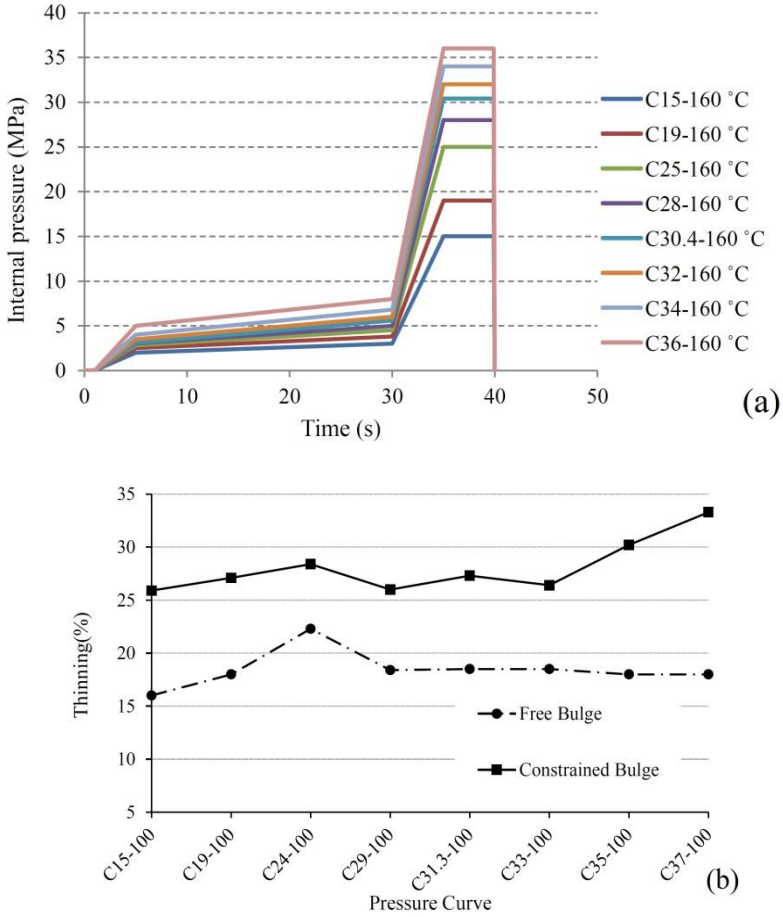


Figure 7. (a) Pressure curve using at 160 ˚C (b) maximum thinning using new pressure curves

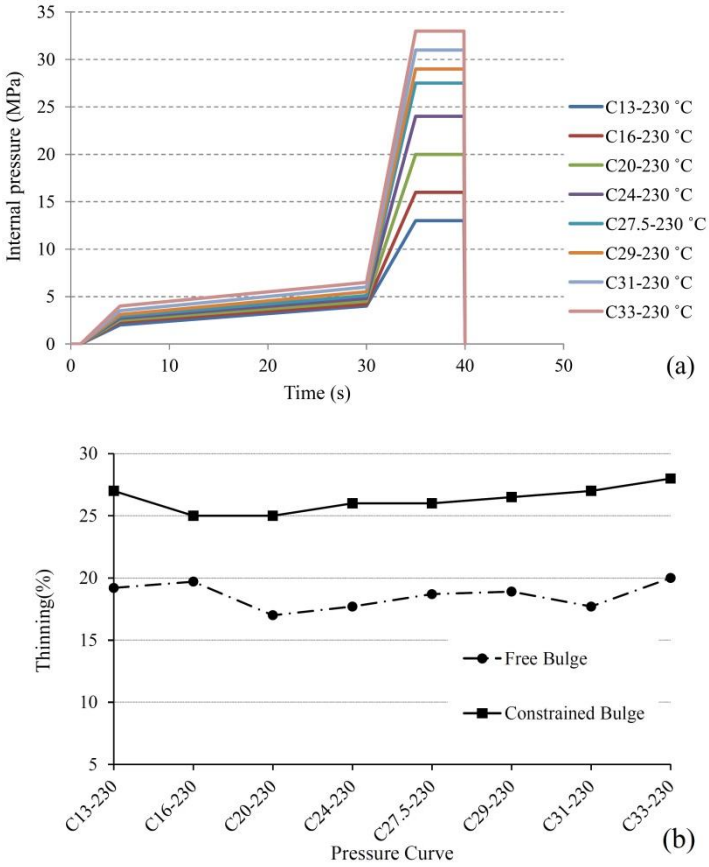


Figure 8. (a) Pressure curve using at 230 ˚C (b) maximum thinning using new pressure curves

Considering selected pressure curves at each temperature, by increasing the temperature of the process, the error of the primary pressure curve will be more. This means, at high temperature, equations (1), (2), and (3) are not suitable for the pressure curve. Also by increasing temperature in free bulge state, thinning decreases but in constrained bulge state, thinning increases at high temperatures.

The formed part at the die corner using the C13-230 pressure curve is shown in Figure 9. As shown, due to low calibration pressure, the tube doesn't fill the die corner.

Finally, axial feeding curves which are shown in Figure 10 (a), are used in simulation to minimize the thinning at 230 ˚C. Among these axial feeding curves, D4 has minimum thinning. If axial feeding is high like D5 and D6 curves, winkling occurs before calibration pressure. A wrinkled part is shown in Figure 10 (b).

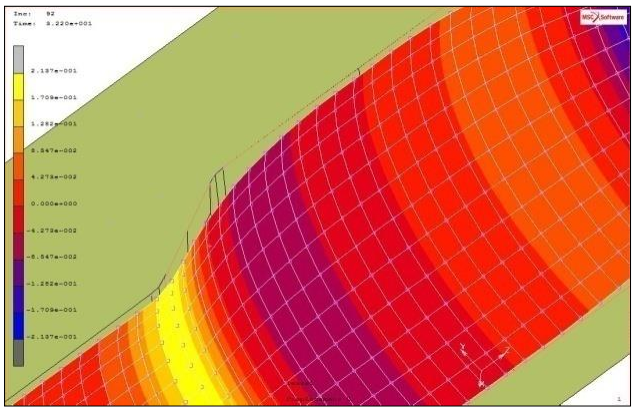

Figure 9. Imperfect part due to low calibration pressure

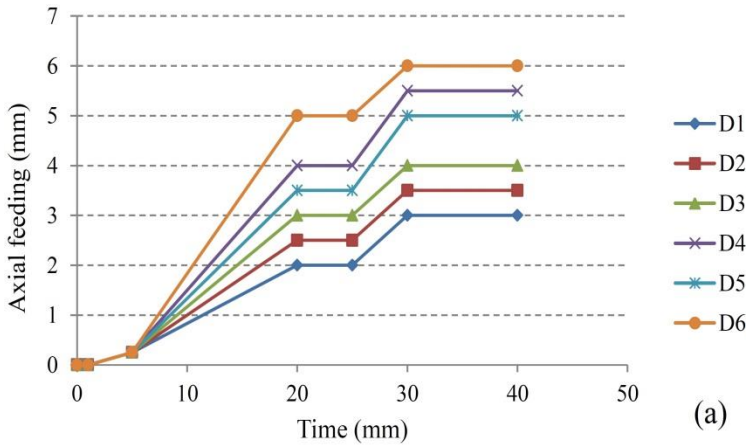


Figure 10. (a) Axial feeding curves (b) wrinkled part

In the experiments, bursting occurred in many samples. The main cause of bursting was a non-uniform distribution of tube thickness in the circumferential direction. Because of the non-uniformity of thickness distribution, the tube bulged asymmetrically. Figure 11 (a) shows an asymmetric bulging. A perfect part is shown in Figure 11 (b).

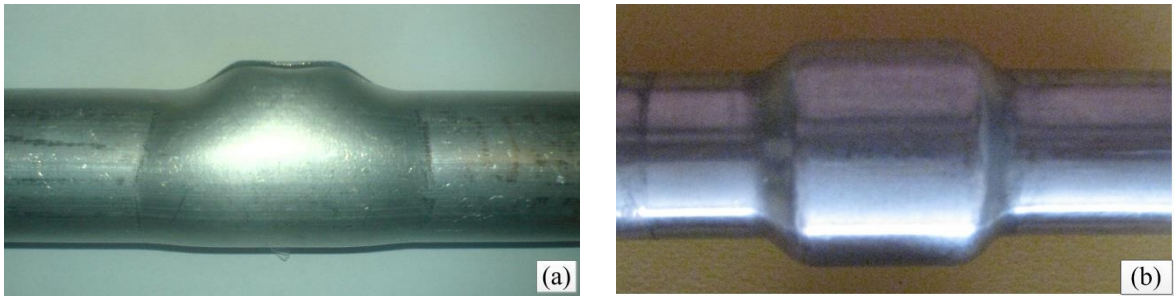

Figure 11. (a) Asymmetric bulging (b) perfect part

## 6. Conclusions

In this paper, warm hydroforming of AA1050 aluminum tubes has been studied numerically and experimentally. Using FEM simulation, an appropriate pressure curve was suggested at three temperatures of 100 ˚C, 160 ˚C, and 230 ˚C. Results showed that thinning decreases at high temperatures when tube ends are free. But when tube ends are constrained, increasing the temperature of the process leads to thinning. Also, non-uniformity of thickness distribution in the circumferential direction can lead to asymmetric bulge and finally bursting in the calibration stage.

## 6. References

[1] Keigler, M., Bauer, H., Harrison, D., Anjali K. and De Silva, M. 2005. Enhancing the formability of aluminium components via temperature controlled hydroforming. Journal of Materials Processing Technology. 167: 363–370.

[2] Yuan, S., Qi, J. and He, Z. 2006. An experimental investigation into the formability of hydroforming 5A02 Al-tubes at elevated temperature. Journal of Materials Processing Technology. 177: 680–683.

[3] Kim, B. J., Van Tyne, C. J., Lee, M. Y. and Moon, Y. H2007. Finite element analysis and experimental confirmation of warm hydroforming process for aluminum alloy. Journal of Materials Processing Technology. 187–188: 296–299.

[4] Yi, H. K., Pavlina, E. J., Van Tyne, C. J. and Moon, Y. H. 2008. Application of a combined heating system for the warm hydroforming of lightweight alloy tubes. Journal of Materials Processing Technology. 203: 532–536.

[5] Hashemi, S. J., Moslemi Naeini, H., Liaghat, G. H., Azizi Tafti, R. and Rahmani, F. 2013. Numerical and Experimental Investigation of Temperature Effect on Thickness Distribution in Warm Hydroforming of Aluminum Tubes. Journal of Materials Engineering and Performance. 22: 57-63.

[5] Koc M. and Altan T. 2002. Prediction of forming limits and parameters in the tube Hydroforming process. International Journal of Machine Tools & Manufacture. 42: 123–138.

[6] Seyedkashi, S.M.H., Naeini, H.M. and Moon, Y.H. 2014. Feasibility study on optimized process conditions in warm tube hydroforming. Journal of Mechenical Sciences Technology. 28: 2845–2852.

[7] Hashemi, S.J., Moslemi Naeini, H., Liaghat, G.H. and Azizi Tafti, R. 2015. Prediction of bulge height in warm hydroforming of aluminum tubes using ductile fracture criteria. Archives of Civil and Mechanical Engineering. 15: 19-29.

[8] Taheri Ahangar, A., Bakhshi-Jooybari, M., Hosseinipour, S. and Gorji, H. 2019. Improvement of Die Corner Filling of Stepped Tubes Using Warm Hybrid Forming. International Journal of Engineering. 32(4): 587-595.

[9] Reddy, P.V., Reddy, B.V. and Ramulu, P.J. 2020. Effect of heat treatment temperatures on formability of SS 304 during tube hydroforming process. SN Applied Sciences. 2(2):1-12.

[10] Zhang, C., Liu, W., Huang, L., Wang, C., Huang, H., Lin, L. and Wang, P. 2021. Process analysis of biconvex tube hydroforming based on loading path optimization by response surface method. The International Journal of Advanced Manufacturing Technology. 112: 2609-2622.

[11] Taheri Ahangar, A., Bakhshi Jooybari, M., Hosseinipour, S. and Gorji, H. 2018. Experimental study and finite element simulation for determining the forming window of 6063-O aluminum tube in warm hydroforming process. Amirkabir Journal of Mechanical Engineering. 52: 571-586.

[12] Nasrollahzade, M., Moslemi Naeini, H., Hashemi, S.J., Abbaszadeh, B. and Shahbazi Karami, J. 2016. Experimental investigation of Aluminum tubes hot gas forming and production of square cross-section specimens. Modares Mechanical Engineering. 15: 435-442.